

Article

Online Recombination Correction in Dosimetry with Arrays of Ionization Chambers: Application to FFF and UHDR Radiotherapy

Juan Pardo-Montero ^{1,2,*} , Jose Paz-Martín ³, Luis Brualla-González ⁴ and Faustino Gómez ^{3,5,*}

- ¹ Group of Medical Physics and Biomathematics, Instituto de Investigación Sanitaria de Santiago (IDIS), 15706 Santiago de Compostela, Spain
 - ² Department of Medical Physics, Complejo Hospitalario Universitario de Santiago de Compostela, 15706 Santiago de Compostela, Spain
 - ³ Department of Particle Physics, Universidade de Santiago de Compostela, 15782 Santiago de Compostela, Spain; jose.martin@usc.es
 - ⁴ ASCIRES Department of Medical Physics, Hospital General Universitario de Valencia, 46014 Valencia, Spain; lbrualla@eres.com
 - ⁵ Group of Molecular Imaging, Instituto de Investigación Sanitaria de Santiago (IDIS), 15706 Santiago de Compostela, Spain
- * Correspondence: juan.pardo.montero@sergas.es (J.P.-M.); faustino.gomez@usc.es (F.G.)

Abstract: Recombination of charge carriers can affect the response of ionization detectors used for the dosimetry of radiotherapy fields. In this work, we present a method for correcting online the recombination effects in arrays of ionization chambers irradiated with time-varying dose rates. The method is based on the characterization of the dose rate/recombination response of the detector, and the measurement of the instant ionization current in the detector, rather than the integrated charge. The proposed method was investigated with simulations of the response of different air and liquid ionization chambers in situations where recombination can be large. In addition, we experimentally investigated the application of the method with an in-house-developed liquid-filled ionization chamber. The proposed online correction method can compensate for recombination losses and seems feasible to implement in the software of ionization arrays/detectors used for the dosimetry of radiotherapy fields.

Keywords: recombination; ionization chamber; FFF; UHDR



Citation: Pardo-Montero, J.; Paz-Martín, J.; Brualla-González, L.; Gómez, F. Online Recombination Correction in Dosimetry with Arrays of Ionization Chambers: Application to FFF and UHDR Radiotherapy. *Appl. Sci.* **2021**, *11*, 10083. <https://doi.org/10.3390/app112110083>

Academic Editors: Cinzia Talamonti, Marco Petasecca and Simona Giordanengo

Received: 24 September 2021
Accepted: 22 October 2021
Published: 28 October 2021

Publisher's Note: MDPI stays neutral with regard to jurisdictional claims in published maps and institutional affiliations.



Copyright: © 2021 by the authors. Licensee MDPI, Basel, Switzerland. This article is an open access article distributed under the terms and conditions of the Creative Commons Attribution (CC BY) license (<https://creativecommons.org/licenses/by/4.0/>).

1. Introduction

Arrays of ionization detectors are an important tool for the quality assurance of radiotherapy treatments and are widely used in radiotherapy quality assurance [1,2]. Several arrays have been developed, relying on different detection technologies like air-filled ionization chambers, solid-state detectors, or liquid-filled ionization chambers [3–13].

Recombination of charge carriers can affect the response of ionization detectors used for the dosimetry of radiotherapy fields. Recombination in air and liquid ionization chambers is well understood, and there exist validated models and correction methods (like the two-voltage-method in air-filled ionization chambers for moderate dose rates) that can be employed to correct the reading of an ionization detector [14,15]. These methods can be applied in static situations when the dose rate in the detector does not change with time.

However, in many clinical situations, the above condition does not hold. When an array of detectors is used to verify a radiation treatment, each detector is irradiated with a varying dose rate depending on the configuration of the fields conforming the treatment. In this situation, recombination cannot be properly corrected. While this may not be an issue when measuring dose distributions in conventional radiotherapy (because of low dose rates and low recombination effects in most detectors), it may have important consequences when measuring treatments delivered by flattening-filter-free (FFF) linacs [16], or ultra-high dose rate (UHDR) radiotherapy [17,18].

In this work, we present a method for correcting online the recombination effects in arrays of ionization chambers irradiated with time-varying dose rates. The method is based on the characterization of the dose rate/recombination response of the detector, and the measurement of the instant ionization current in the detector, rather than the integrated charge. Recombination in ionization chambers irradiated with dynamic fields has been studied by other authors. In particular, Boag theoretically studied recombination in an ionization chamber irradiated by a swept beam [19]. Palmans et al. studied recombination in ionization chambers irradiated by Tomotherapy dynamic beams and developed a dynamic method of correction based on the calculation (with Monte Carlo) and integration of dynamic dose rates in the detector [20].

2. Methods and Materials

2.1. Online Correction Method: Pulsed Radiation

2.1.1. Recombination in Pulsed Beams

The collection efficiency of a radiation detector irradiated with a pulsed beam is well described by the equation of Boag in the near-saturation regime ($f > 0.9$) [21]:

$$f = \frac{1}{u} \log(1 + u) \quad (1)$$

The variable u depends on the polarization voltage, V , dose per pulse, D_0 , and the geometry and properties of the sensitive material. We can just summarize this dependence as,

$$u \sim \frac{c}{V} \quad (2)$$

where c is proportional to D_0 .

Equations (1) and (2) are behind the development of the two-voltage-method for air-filled detectors irradiated with pulsed beams [20,22]. In the case of liquid-filled detectors, the ionized charge per pulse depends on the applied voltage due to initial recombination, and more complex methodologies are necessary to obtain the collection efficiency [14,15,23].

In the case of a significant contribution of free electrons to the collected charge, the following could be used alternatively [24]

$$f = \lambda + \frac{1}{u} \log \left[1 + \frac{e^{\lambda(1-\lambda)u} - 1}{\lambda} \right] \quad (3)$$

with $\lambda = 1 - \sqrt{1 - p}$, and p the free-electron fraction in the chamber.

2.1.2. Analytic Online Correction Method—Pulsed Beams

In a pulsed beam with period T and dose per pulse D_0 , we can define the average dose rate as:

$$\langle \dot{D} \rangle = \frac{D_0}{T} \quad (4)$$

Equally, we can define the average ionization current associated with the full charge collected without recombination effects:

$$\langle I \rangle = \frac{e D_0 m}{W T} \quad (5)$$

where e stands for the elementary charge, m is the mass of the active volume of the chamber and W is the average energy per electron–ion pair released in the medium.

The chamber actual average electrical current can be obtained through the integration in a time interval of duration Δt in the form:

$$\langle I_{col}(t) \rangle = \frac{1}{\Delta t} \int_t^{t+\Delta t} I_{col}(t) dt \quad (6)$$

where $I_{col}(t)$ is the actual instantaneous readout current. This moving average value, $\langle I_{col}(t) \rangle$, can suffer fluctuations depending on the size of the time integration interval Δt , the actual shape of the instantaneous current of the detector after each pulse, and due to variations in time of the irradiation delivery (i.e., dose per pulse and pulse repetition rate). However, if Δt is sufficiently large compared with pulse period T , and considering that irradiation conditions are steady during that interval, the relative standard deviation of $\langle I_{col}(t) \rangle$ could be reasonably small for the application of the method proposed in this work. For example, taking $\Delta t \geq 50T$ provides a standard deviation for $\langle I_{col}(t) \rangle$ below 1%.

Under these conditions, we may assume that for a given average ionization current $\langle I \rangle$ there is an associated charge collection efficiency $f(\langle I \rangle)$, and thus we can write that

$$\langle I_{col} \rangle \approx f(\langle I \rangle) \cdot \langle I \rangle \quad (7)$$

where $f(\langle I \rangle)$ is the collection efficiency associated to the ionization current $\langle I \rangle$, which is proportional to the dose rate in the detector, $\langle \dot{D} \rangle$.

We can use the two-voltage method, or any other method, to determine the collection efficiency at a reference dose per pulse, D_0^{ref} , or, equivalently, at a given ionization reference current $\langle I_{ref} \rangle$. We will denote the value of u in this reference condition as u_{ref} . Then, the variable u at a different dose per pulse D_0 verifies that:

$$\frac{u}{u_{ref}} = \frac{D_0}{D_0^{ref}} = \frac{\langle I \rangle}{\langle I_{ref} \rangle} \quad (8)$$

consequently,

$$f(\langle I \rangle) = \frac{\langle I_{ref} \rangle}{u_{ref} \langle I \rangle} \log \left[1 + u_{ref} \frac{\langle I \rangle}{\langle I_{ref} \rangle} \right] \quad (9)$$

From Equation (7), we can express $\langle I \rangle$ as

$$\langle I \rangle \approx \frac{\langle I_{col} \rangle}{f(\langle I \rangle)} \quad (10)$$

and substituting in Equation (9), we can obtain

$$f(\langle I \rangle) \approx \frac{\langle I_{ref} \rangle f(\langle I \rangle)}{u_{ref} \langle I_{col} \rangle} \log \left[1 + u_{ref} \frac{\langle I_{col} \rangle}{\langle I_{ref} \rangle f(\langle I \rangle)} \right] \quad (11)$$

We can solve the above equation for $f(\langle I \rangle)$ to obtain:

$$f(\langle I \rangle) \approx \frac{u_{ref} \langle I_{col} \rangle}{\langle I_{ref} \rangle \left[\exp \left(\frac{\langle I_{col} \rangle u_{ref}}{\langle I_{ref} \rangle} \right) - 1 \right]} \quad (12)$$

This expression can be used to correct online the readout signal. The correction factor only depends on the own value of $\langle I_{col} \rangle$ and a single parameter, $k_{ref}^p = u_{ref} / \langle I_{ref} \rangle$, which can be experimentally determined. Thus, we can write that:

$$f(\langle I \rangle) \approx \frac{k_{ref}^p \langle I_{col} \rangle}{\exp \left(k_{ref}^p \langle I_{col} \rangle \right) - 1} \quad (13)$$

$$\langle I_{corrected}(t) \rangle \approx \frac{\langle I_{col} \rangle}{f(\langle I \rangle)} \quad (14)$$

2.1.3. Considerations Regarding the Application to Liquid-Filled Ionization Chambers

In order to apply Boag's Equation (1) (and correction methods based on it), there must be no overlapping between charges ionized by consecutive pulses, i.e., charge collection must take less than the time between consecutive pulses. This constraint is easily satisfied in air-filled chambers, where the mobilities of charge carriers are large. However, this may not be the case in liquid-filled detectors, where charge collection takes ~ 10 ms operating under standard conditions, while the time between pulses may be below that value in clinical LINACs.

However, even if Boag theory cannot be formally applied, it was shown in [25] that the functional dependence of the collection efficiency on the dose per pulse does not change with overlapping. In this situation, in the near-saturation region we can write:

$$f = \frac{1}{u'} \log(1 + u') \quad (15)$$

where $u' \sim D_0$.

Because the functional dependence of the collection efficiency on the dose per pulse does not change, correction methods based on this dependence, like the two-dose-rate method [14], can still be employed. This is not the case with correction methods based on the functional dependence of the collection efficiency on the voltage (like the three-voltage method [23]). The online correction method developed in the previous section can also be applied, with the particularity that the two-dose-rate method is used to obtain the value of u'_{ref} .

A further consideration needs to be taken into account in LICs, regarding the extended collection time of the charge released by a pulse and the integration time. As mentioned in the above discussion, the charge collection time in LICs is not negligible in comparison with the time between pulses (in fact, it may be larger). In addition, due to the high density of the ionization medium, the readout signal is large, and integration times may be limited to values of the order of ms (depending on the readout electronics). As the integration time, the collection time, and the time between pulses are of the same order of magnitude, fluctuation on the readout signal may appear which are not caused by variations of the dose per pulse (this is easily noticeable in Section 3.1 for measurements taken with the detector presented in [13]). Such fluctuations, which are not caused by variations of the dose per pulse, should be minimized to improve the accuracy of the online correction method. As discussed in Section 2.1.2, one should set $\Delta t \gg T$ to avoid this issue. If this is not technically possible, replacing the readout current ($\langle I_{col} \rangle$) with a moving average, $\langle I_{MA,n} \rangle$ (emulating a longer integration time), will reduce the undesired fluctuations:

$$\langle I_{MA,n}(t_i) \rangle = \left(\sum_{j=i-n+1}^i \langle I_{col}(t_j) \rangle \right) / n \quad (16)$$

This moving average will be used in the analysis of experimental data of a LIC in Section 3.1.

2.2. Online Correction Method: Continuous Radiation

2.2.1. Recombination in Continuous Beams

Nowadays, continuous radiation is far less used than pulsed radiation in radiotherapy. Nonetheless, we shall present the method for continuous beams (e.g., cobalt-60 units) for the sake of completeness. In this situation, the method becomes simpler, because there is no need for averaging to counteract the pulsed structure of the beam. The collection efficiency of a radiation detector irradiated with continuous radiation is well described by the Greening formula [26,27] when $f > 0.9$:

$$f = \left(1 + \frac{a}{\sqrt{2}} \right)^{-1} = (1 + b)^{-1}, \quad (17)$$

where V is the polarization voltage, and a is a parameter that depends on the physicochemical properties of the ionization medium and is proportional to the dose rate, \dot{D} . The first expression shows the explicit dependence on the polarization voltage, but for the purpose of this work, the second expression, with $b = a/V^2$, is more adequate.

This equation has been used to develop recombination correction methods in static situations, like the very well known two-voltage method for gas ionization chambers in continuous beam [20,28,29], and the three-voltage and two-dose rate methods in LICs [23,30].

2.2.2. Analytic Online Correction Method—Continuous Beams

We define the ionization current $I(t)$ in this case as:

$$I(t) = \frac{e \dot{D} m}{W} \quad (18)$$

We will assume that the variations in time of the dose rate \dot{D} are sufficiently slow as to keep the equilibrium charge carrier distributions across the detector at each time t .

The current in the detector is given by:

$$I_{col}(t) = I(t) f(I(t)), \quad (19)$$

where $I_{col}(t)$ is the readout current, $I(t)$ is the ionization current, and f the collection efficiency. As $\dot{D}(t) \propto I(t)$, we can write the collection efficiency as a function of $I(t)$.

We can use the two-voltage-method, or any other method, to determine the collection efficiency at a reference dose rate, $\dot{D}_{ref} \sim I_{ref}$, and the value of b , which we will refer to as $b(\dot{D}_{ref}) \equiv b(I_{ref}) \equiv b_{ref}$. The collection efficiency at any other dose rate/ionization current can be written as:

$$f(I(t)) = \left(1 + b_{ref} \frac{I(t)}{I_{ref}} \right)^{-1} \quad (20)$$

$I(t)$ is not known, but $I_{col}(t)$ is measured, and by using Equation (19) we can write:

$$f(I(t)) = \left(1 + b_{ref} \frac{I_{col}(t)}{I_{ref} f(I(t))} \right)^{-1} \quad (21)$$

This equation can be solved to obtain an expression for the collection efficiency as a function of the measured ionization current $I_{col}(t)$:

$$f(I(t)) = \left(1 - \frac{b_{ref} I_{col}(t)}{I_{ref}} \right) = (1 - k_{ref}^c I_{col}(t)) \quad (22)$$

where $k_{ref}^c = b_{ref}/I_{ref}$ in continuous irradiation. With this expression, we can correct the readout current as:

$$I_{corrected}(t) = \frac{I_{col}(t)}{f(I(t))} \quad (23)$$

2.3. Correction Methods beyond Boag and Greening Limits

In the previous two sections, we developed the online correction method from the analytic expressions of Boag and Greening for pulsed and continuous beams, respectively. We obtained simple closed-form expressions for the proposed correction method. However, in many experimental situations, the expressions presented above do not hold. For example, in gas-filled ionization chambers, it is customary to include the effects of initial recombination and recombination by diffusion in the overall collection efficiencies [20,29], even though these contributions are smaller than general/volume recombination. Additionally, in gas chambers, charge multiplication may play a role too, and it should be considered when analyzing the response of the chamber [20]. The addition of these terms

will lead to modifications of the methods presented above, but the methodology would remain the same.

More interestingly, in situations where dose rates/doses per pulse are very large, volume recombination can be quite important, and the Boag/Greening analytic expressions will fail to describe the dependence of the collection efficiency on the dose rate/dose per pulse. Those expressions are only valid in the *near-saturation* region, with $f > 0.9$. This may be the case in FFF radiotherapy, with doses per pulse reaching ≈ 2 mGy, and especially UHDR radiotherapy, with doses per pulse that can be several orders of magnitude higher. In these situations, the densities of charge carriers in the ionization medium are much larger, field screening effects become important, and the analytic description of the collection efficiency is no longer valid.

However, in this situation, the dependence of the collection efficiency on the dose per pulse (ionization current) can be characterized experimentally,

$$f(I) = g(\{a_i\}, I) \quad (24)$$

where $\{a_i\}$ are a set of parameters that describe the dependence (they can arise from an interpolation of experimental data, or from a phenomenological function fitting the dose per pulse dependence, as in [31]). After the collection efficiency is accurately characterized (i.e., the function g is known, either analytically or numerically), the collection efficiency can be obtained following the procedure described in the previous section, by writing the equation as

$$f(I) = g(\{a_i\}, f(I)I_{col}) \quad (25)$$

and solving for $f(I)$.

2.4. Experimental Data

The presented methods were applied to measurements taken with the liquid-filled ionization chamber presented in [13]. This array has 2041 detectors with 2.5×2.5 mm² effective area and 0.5 mm thickness. A total of 43×43 detectors cover a central area of 107.5×107.5 mm². The operation voltage is +1500 V, yet, despite this operation voltage, recombination is still important for large dose rates [13,25]. The readout is done with VLSI electrometers (Sens-Tech Ltd, Egham, UK), which communicate with a computer through an Ethernet interface. The readout can be performed at rates >1000 Hz, even though in practice we usually employed values of 20–250 Hz (4 to 50 ms integration times). The readout software includes an option (*sequence mode*) that allows saving every single acquisition, in addition to the total integrated signal.

Measurements were performed at Hospital General de Valencia-ERESA in a True-beam linear accelerator (Varian Medical Systems, Palo Alto, CA, USA). We analyzed the verification of a complex treatment, a lymph node tumor treatment consisting of 15 fields. The treatment was delivered at 600 MU/min. The acquisition was saved in *sequence mode* and analyzed offline (the online correction method was not implemented in the readout software) to correct for recombination with the proposed method.

2.5. Numerical Simulations

We further investigated the application of the proposed methods by performing numerical simulations of the response of both air-filled ionization chambers and liquid-filled ionization chambers to a time-varying dose rate irradiation. We have used an in-house developed software that numerically solves the transport equations of charge carriers in an ionization detector. The software has been validated in previous publications [23,25]. The main parameters included in the simulation are presented in Table 1. The detectors that we have simulated correspond to the LIC presented in [13], and the PTW “729” and “1500” arrays [9]. We would like to note here that there are different versions of the 729 detector, which operate at different voltages. We have simulated the detector operating at 400 V, as shown in Table 1.

The dose-rate profile of the irradiation was taken from the clinical lymph node treatment presented in Section 2.4. This clinical treatment delivers a maximum dose per pulse of ~ 0.5 mGy. For the simulation study, the dose per pulse in each segment was scaled up (and the irradiation time scaled down accordingly) to reach maximum values of 1 mGy, 2 mGy and 50 mGy while keeping constant the total dose delivered. This was done to explore dose per pulse regimens with high recombination. The first two values correspond to typical dose per pulse values encountered in FFF radiotherapy, while the latter corresponds to values encountered in UHDR radiotherapy.

Table 1. Main characteristics and physical parameters of the simulated detectors. LIC corresponds with the isoctane-filled liquid ionization chamber presented in [13], while PTW729 and PTW1500 correspond with the pixel characteristics of the air-filled PTW “729” and “1500” arrays [9].

Parameter	Detectors		
	LIC	PTW729	PTW1500
Pixel gap (mm)	0.5	1	1
Polarization voltage (V)	1000–1500	400	1000
Ion mobilities ($\text{m}^2 \text{V}^{-1} \text{s}^{-1}$)	$2.3\text{--}3.5 \times 10^{-8}$	$1.18\text{--}1.44 \times 10^{-4}$	$1.18\text{--}1.44 \times 10^{-4}$
Electronic mobilities ($\text{m}^2 \text{V}^{-1} \text{s}^{-1}$)	-	0.1504	0.0751
G_{fi} (ionization pairs/(100 eV))	0.69 (@1000 V)–0.88 (@1500 V)	2.94	2.94

3. Results

3.1. Correction of the Readout of a LIC: Experimental Data and Simulations

In Figure 1 we present the readout current versus time in a certain pixel of the LIC used to verify the lymph node tumor treatment delivered at 600 MU/min presented in Section 2.4 (*sequence mode* acquisition). The variation of dose rate in the pixel is easily noticeable, with segments *missing* the pixel and delivering no dose other than scatter, and other segments clearly irradiating the pixel. Fluctuations in the readout signal associated to each segment are easily noticeable in Figure 1. Such fluctuations are caused by the collection time of the ionized charge rather than by intrinsic fluctuations of the dose per pulse (Section 2.1.3). The spikes noticed at the beginning of several segments may be an exception. The origin of such spikes is not clear: it may be an overshoot of the LINAC at the start of the delivery, which is then adjusted by the feedback circuit, or it may be caused by the response of the readout electronics. In order to minimize such fluctuations, a moving average was used.

The correction method was applied to this set of data. Firstly, the dependence of the collection efficiency with the dose per pulse was investigated [14,25], in order to obtain the parameters needed to apply the correction method of Equation (12). It is important to notice that when irradiating the LIC at 600 MU/min, the Boag condition of no superposition of charge carriers ionized by different pulses does not hold (this is noticeable in the signal structure of Figure 1). However, as discussed in Section 2.1.3, we can still apply the correction formalism presented in this work. The reference dose per pulse for these calculations was 1 mGy, which results in a value $u_{ref} = 0.090$ (collection efficiency 0.958).

The effect of the correction is shown in Figure 2. We present the 2D map of the integrated signal for the treatment delivered at 600 MU/min (panel A) to show the shape of the dose distribution. The correction method is applied to each pixel, and it leads to an increase of the readout current, especially noticeable when the dose per pulse is high, as shown in panel C for a pixel of the detector. The overall effect of the correction method is an increase of the integrated signal up a $\sim 3\%$, which is consistent with the recombination loss at this dose rate in this detector [25]. This is illustrated in panel B for a profile of the integrated signal.

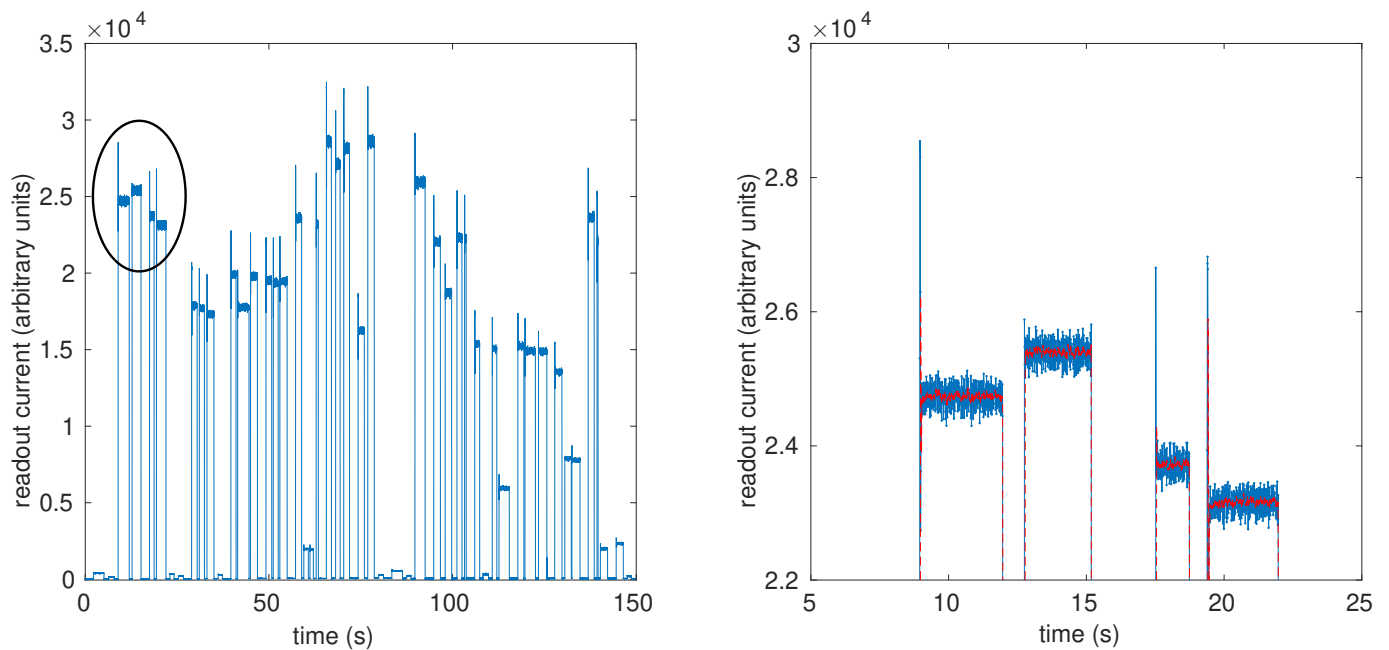


Figure 1. Ionization current in a pixel of a liquid-filled ionization chamber during the verification of a clinical radiotherapy treatment delivered at 600 MU/min. The many segments composing the treatment are easily spotted in the (left) panel. The (right) panel shows a zoom-in of the region highlighted within the ellipse shown in the (left) panel, and illustrates the effect of the moving average procedure (Equation (16) with $n = 10$): moving average (red line), raw data (blue line).

The effect of recombination in LICs was further explored with simulations. In particular, the spatiotemporal dose-rate profile of the verified treatment was converted to simulate a delivery at a monitor unit rate of 2400 MU/min (2.8 ms between consecutive pulses) and a maximum dose per pulse of 2 mGy (roughly corresponding to a delivery at 10 MV-FFF in a TrueBeam linac). In order to speed up the simulation, the time distance between segments (with no irradiation) was reduced to 0.1 s. In Figure 3 we show the profile of the readout signal for a particular pixel operating at 1000 V, as well as the corrected signal according to the online recombination method (Equations (12) and (13)). The reference dose per pulse for these calculations was 1 mGy, which results in a value $u_{ref} = 0.146$ (collection efficiency 0.933). The raw integrated current in this case amounts to 91.5% of the ionization current (i.e., 8.5% of the generated charge is lost to recombination). On the other hand, the corrected integrated current amounts to 99.5% of the ionization current. Therefore, even in this situation of very large recombination, the online recombination methods seem to work quite well, the residual 0.5% difference between corrected and generated signal arising from departures from Boag formula for collection efficiencies below $\simeq 0.9$.

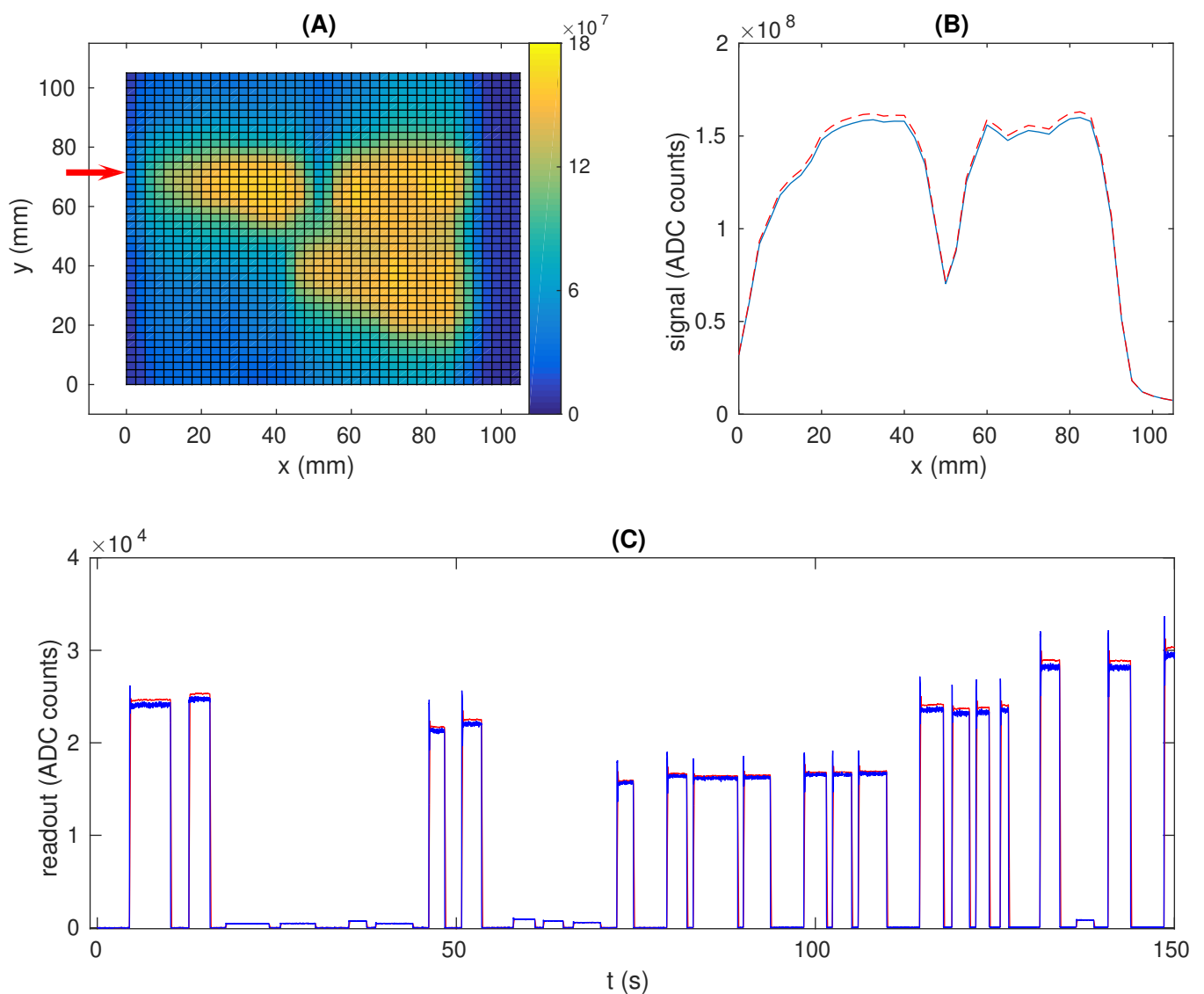


Figure 2. Effect of recombination and recombination correction in the verification of a dynamic radiotherapy clinical treatment with a liquid-filled ionization chamber array of 43×43 pixels of $2.5 \text{ mm} \times 2.5 \text{ mm}$ each. (A) Raw acquisition with a LINAC monitor unit rate of 600 MU/min. (B) Representative profiles (along the line highlighted in panel (A) with a red arrow) of the raw (solid line) and corrected (dashed line) acquisitions. (C) Profile of the raw readout current in a pixel of the detector (blue line) and the corrected readout (red line).

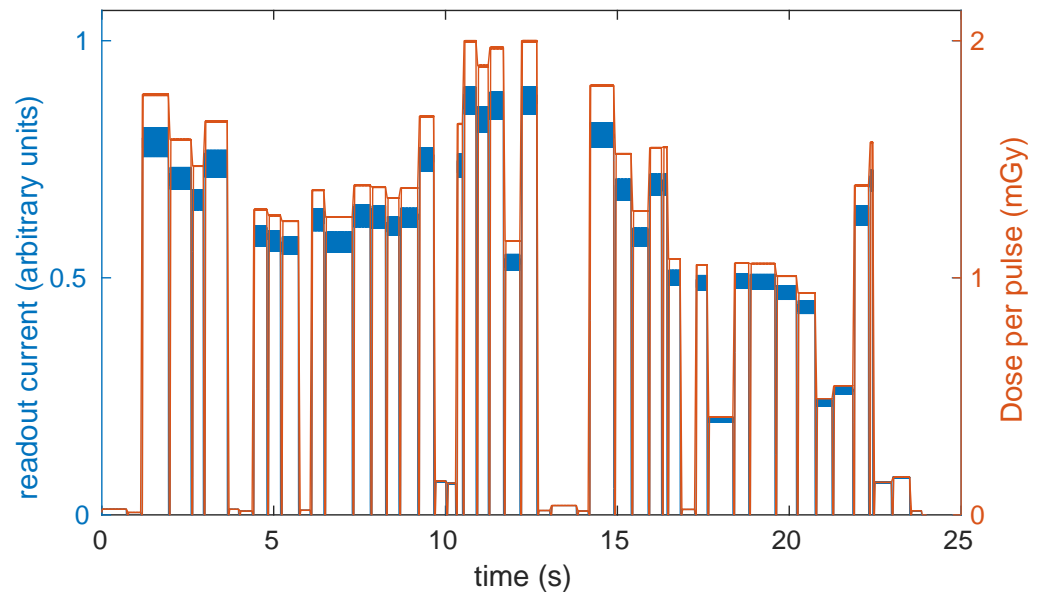


Figure 3. Simulated readout signal in a pixel of the LIC operating at 1000 V and irradiated by a beam simulating a delivery with a maximum dose per pulse of 2 mGy (roughly corresponding to a delivery at 10 MV-FFF in a TrueBeam linac) and 2.8 ms between pulses (blue line). The corrected signal is also shown (red line), as well as the variation of the dose per pulse during the irradiation. It is observed that the larger the dose per pulse, the more important the difference between raw readout and collected readout (due to increased recombination).

3.2. Simulations of the Response of Air-Filled Ionization Chamber

The simulations show that recombination in air ionization chambers with the characteristics of the PTW1500 is not very important for the verification of treatments delivered at doses per pulse of 1 mGy and 2 mGy (typical values employed in FFF radiotherapy). This is illustrated in Figure 4A,B, for a particular position (pixel) in the radiation treatment field. This response is in agreement with the results published in [9] for this detector, which was specifically designed to prevent recombination issues in FFF deliveries. When the maximum dose per pulse is increased to 50 mGy (a value that is not representative of FFF, but closer to those employed in intraoperative radiation therapy (IORT) deliveries), recombination losses become more important, and the Boag formalism shows a clear overestimation of the collection efficiency. The reference dose per pulse for these calculations was 1 mGy, which results in a value $u_{ref} = 0.008$ (collection efficiency 0.996).

The results for the air ionization chambers with the characteristics of the PTW729, shown in Figure 5, illustrate a greater impact of volume recombination. The reference dose per pulse for these calculations was 1 mGy, which results in a value $u_{ref} = 0.069$ (collection efficiency 0.967). The developed method is able to correct for these effects and reproduce the total integrated charge in the case of 1 mGy and 2 mGy. However, at 50 mGy per pulse, the correction overestimates the real signal as in the case of PTW1500-like air-chamber. The overestimation effect is visibly higher for the case of the PTW1500 detector since the contribution of free electrons is considerably greater (due to lower gap and higher voltage). Therefore, in situations where the collection efficiency departs from the Boag formula, it would be convenient to correct with the model of Equation (3), or a phenomenological characterization of the dependence of the collection efficiency on the dose per pulse, as in Equation (24).

It should be noted that the integration time in the 1 mGy and 2 mGy cases was set to 200 ms for both chamber types. However, this is not the case for the 50 mGy simulation, where, as the treatment is scaled so that the total dose is maintained, the number of pulses for each configuration is significantly lower. Thus, for this case, the integration time was set to 2.7 ms, a value similar to the distance between pulses, in order to be able to apply the method correctly.

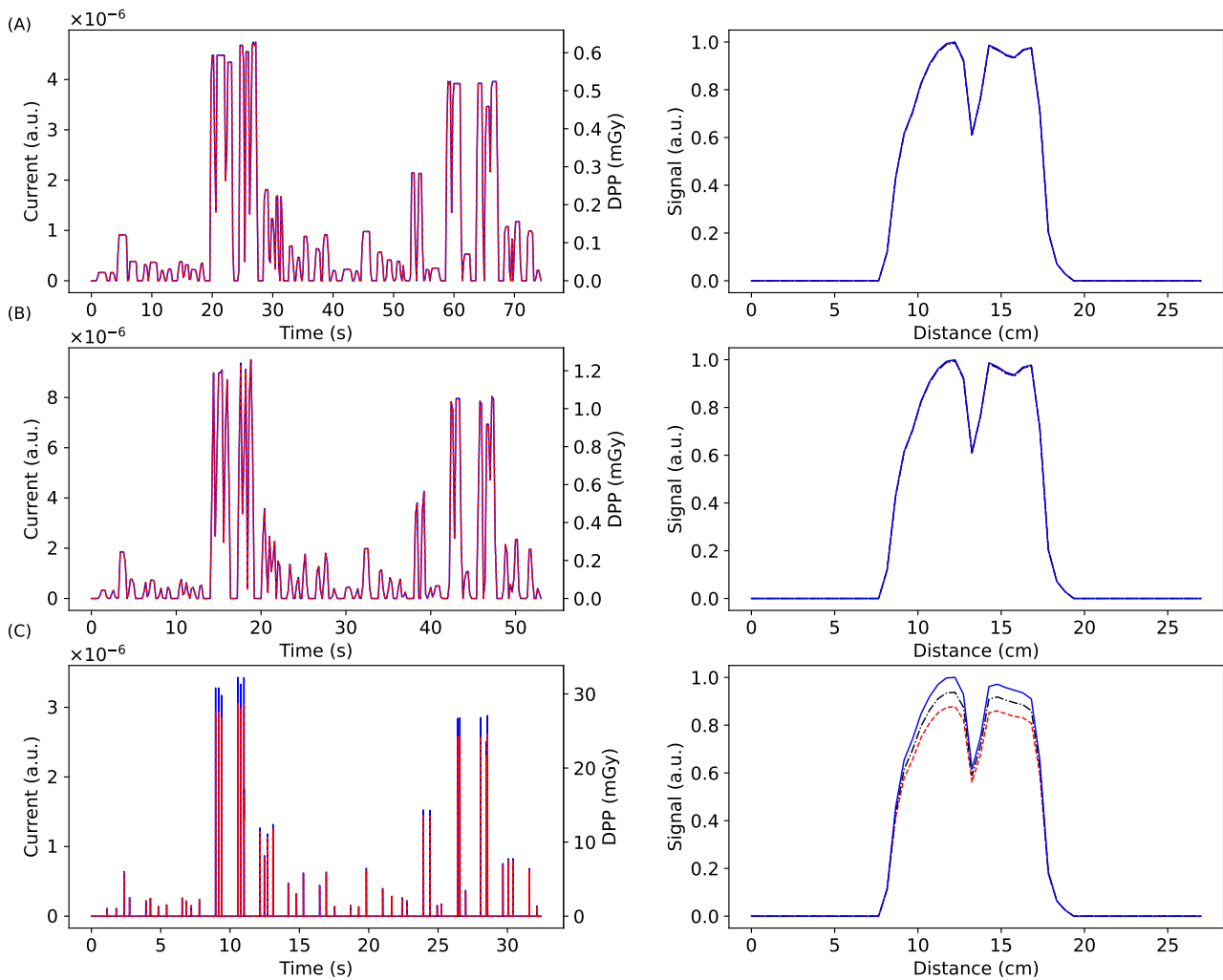


Figure 4. Effect of recombination and recombination correction in the verification of a dynamic radiotherapy clinical treatment with a PTW1500-like air-chamber. The dynamic dose rate corresponds to that of a lymph node tumor treatment, but scaled up to deliver a maximum dose per pulse of 1 (A), 2 (B) and 50 mGy (C). In the left panels we show for a particular pixel the raw readout current (red lines) and corrected readout current (blue lines) versus time. Notice that the dose per pulse in this pixel does not reach the maximum dose per pulse of the delivery. In the right panels we show a profile of the radiation field (the one shown in Figure 2), including generated charge (solid line), raw collected charge (dashed line), and corrected charge (dash-dot line).

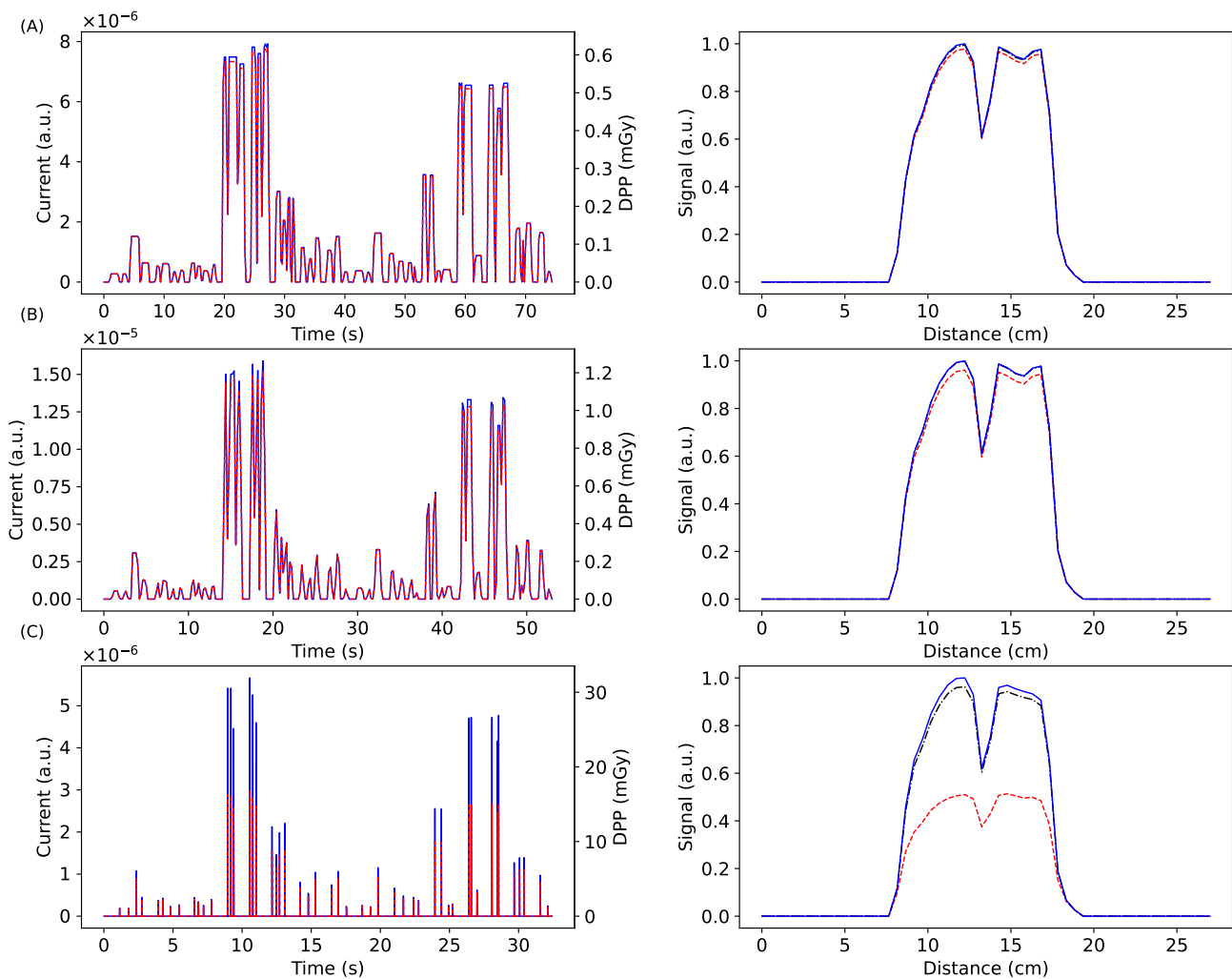


Figure 5. Effect of recombination and recombination correction in the verification of a dynamic radiotherapy clinical treatment with a PTW729-like air-chamber. The dynamic dose rate corresponds to that of a lymph node tumor treatment, but scaled up to deliver a maximum dose per pulse of 1 (A), 2 (B) and 50 mGy (C). In the left panels we show for a particular pixel the raw readout current (red lines) and corrected readout current (blue lines) versus time. Notice that the dose per pulse in this pixel does not reach the maximum dose per pulse of the delivery. In the right panels we show a profile of the radiation field (the one shown in Figure 2), including generated charge (solid line), raw collected charge (dashed line), and corrected charge (dash-dot line).

4. Discussion

In this work, we have presented a method for real-time recombination correction in the dosimetry of dose rate varying radiotherapy treatments with arrays of ionization chambers. The method is based on the measurement of the instantaneous readout current (rather than only the total integrated charge) and the automatic correction according to such measurements. We have investigated the application of the method both with simulations of the response of ionization detectors (liquid- and air-filled chambers) and with preliminary experimental measurements taken with a liquid-filled ionization chamber, showing that the method seems feasible and accurate for the correction for recombination in dose-rate-varying radiotherapy verifications. Nonetheless, further experimental validation of this method is necessary to properly implement this methodology, in particular in different dose-per-pulse/dose-rate regimes and with different detection technologies.

The method presented in this work can be used to correct the readout current in real time, without the need to save large amounts of data to perform the correction offline. This would require to perform the correction operation at a maximum frequency of \simeq kHz.

While in this work we did not perform the correction of the experimental data online, as the online recombination method was not implemented in the readout software at the time when the measurements were performed, we verified at a later stage that performing such operation online, at a frequency of 100–250 Hz is feasible with the software running on a standard personal computer.

The analytic method that we developed for pulsed beams, based on Boag formula, seems adequate for correcting in the near saturation region (collection efficiencies $\simeq 0.9$ or higher). This range includes most applications in conventional radiotherapy and FFF radiotherapy, both for liquid- and air-filled ionization chambers). For UDHR deliveries, where collection efficiencies can be well below the near-saturation region, Boag theory may not be reliable, and it may be necessary to use different parametrizations, as in Equation (3) or Equation (24). In addition, the pulse structure of UHDR deliveries may be quite different to the pulse structure used in conventional/FFF radiotherapy (which we have used in this work). In such situations, it is important to pay special attention to the selection of the integration time of the detector to avoid fluctuations and pulse overlapping. This issue has not been fully investigated in this work due to the lack of realistic delivery sequences for UHDR treatments.

The methods that we propose in this work are similar to those described in [20], where the authors studied recombination in ionization chambers irradiated by dynamic Tomotherapy beams. They considered not only the temporal variation of the dose rate on the detector, but also the spatial variation of the dose rate (caused by dose gradients especially in the penumbra of the beams). However, in that paper, the authors relied on a Monte Carlo calculation of the dose rate on the detector, rather than on the measurement of the ionization current, which allows us to develop an online correction method like the one that we present in this paper. The effect of dose gradients on the volume of the detectors is ignored in this work. In particular, in the analyzed experimental data, the small pixel size ($2.5 \times 2.5 \text{ mm}^2$) should minimize this effect. Nonetheless, the dose-gradient in each detector of an array can be inferred from the measurement of the detectors in its neighborhood, opening the door for the real-time correction of this effect if necessary. However, this was beyond the scope of this work, where we have focused on the correction for recombination. The latter effect is bound to be more important when performing measurements at large dose rates/doses per pulse.

The method proposed in this work may improve the dosimetry of radiotherapy treatments with ionization chamber arrays. The potential is limited for air ionization chambers in conventional and FFF radiotherapy, because such detectors can be designed to present negligible recombination effects. This is not the case with LICs, where recombination losses in FFF radiotherapy can easily reach $\sim 3\text{--}5\%$. Therefore, the correction of that effect can allow to obtain better agreements in relative dosimetry measurements (the normalization of the dose distribution to the maximum/reference dose would perturb the low-dose regions and the penumbra of the dose distributions). In addition, this would allow to perform accurate absolute dosimetry comparisons, rather than relying on relative dosimetry.

Where this method may offer the most potential is in the verification of UHDR treatments, as it would facilitate the use of ionization chamber arrays in a situation where extremely high doses per pulse would limit the application on these devices. There is a need to develop novel methodologies for the dosimetry of UHDR beams (for example, the AAPM has recently established a task force to deal with this issue). The application in such situations will still require more experimental and simulation studies, paying special attention to the pulse structure of those beams. Such detailed studies were beyond the scope of this work, which has been focused on presenting the method. Future studies of the application to UHDR deliveries will be carried out with specific experimental data.

5. Conclusions

We have presented a method for the real-time recombination correction in dosimetry with arrays of ionization chambers. This method may improve the verification of radiotherapy treatments with arrays of ionization chambers, especially in applications where high dose rates are delivered and recombination is large. The correction of recombination effects can allow to obtain better agreements between planned and measured dose distributions. There is a trend towards increasing the dose rate/dose per pulse of radiotherapy treatments, like in FFF and FLASH radiotherapy, and the method that we have presented may facilitate the accurate dosimetry of such radiotherapy treatments with widely used ionization arrays.

Author Contributions: Conceptualization, F.G., J.P.-M. (Juan Pardo-Montero); methodology, J.P.-M. (Jose Paz-Martín), F.G. and J.P.-M. (Juan Pardo-Montero); software, J.P.-M. (Jose Paz-Martín), F.G. and J.P.-M. (Juan Pardo-Montero); validation, J.P.-M. (Jose Paz-Martín), L.B.-G., F.G. and J.P.-M. (Juan Pardo-Montero); formal analysis, J.P.-M. (Jose Paz-Martín), L.B.-G., F.G. and J.P.-M. (Juan Pardo-Montero); investigation, J.P.-M. (Jose Paz-Martín), L.B.-G., F.G. and J.P.-M. (Juan Pardo-Montero); resources, F.G. and J.P.-M. (Juan Pardo-Montero); data curation, J.P.-M. (Jose Paz-Martín), F.G. and J.P.-M. (Juan Pardo-Montero); writing—original draft preparation, J.P.-M. (Jose Paz-Martín), F.G. and J.P.-M. (Juan Pardo-Montero); writing—review and editing, J.P.-M. (Jose Paz-Martín), F.G., L.B.-G. and J.P.-M. (Juan Pardo-Montero); visualization, J.P.-M. (Jose Paz-Martín), F.G. and J.P.-M. (Juan Pardo-Montero); supervision, F.G. and J.P.-M. (Juan Pardo-Montero); project administration, F.G. and J.P.-M. (Juan Pardo-Montero); funding acquisition, J.P.-M. (Juan Pardo-Montero) All authors have read and agreed to the published version of the manuscript.

Funding: This project has received funding from the Instituto de Salud Carlos III (PI17/01428 grant, FEDER co-funding).

Institutional Review Board Statement: Not applicable.

Informed Consent Statement: Not applicable.

Data Availability Statement: Data supporting the reported results are available from the corresponding authors on a reasonable request.

Conflicts of Interest: The authors declare no conflict of interest. The funders had no role in the design of the study; in the collection, analyses, or interpretation of data; in the writing of the manuscript, or in the decision to publish the results.

References

1. Klein, E.E.; Hanley, J.; Bayouth, J.; Yin, F.F.; Simon, W.; Dresser, S.; Serago, C.; Aguirre, F.; Ma, L.; Arjomandy, B.; et al. Task Group 142 report: Quality assurance of medical accelerators. *Med. Phys.* **2009**, *36*, 4197–4212. [[CrossRef](#)] [[PubMed](#)]
2. Kron, T.; Lehmann, J.; Greer, P.B. Dosimetry of ionising radiation in modern radiation oncology. *Phys. Med. Biol.* **2016**, *61*, R167. [[CrossRef](#)]
3. Amerio, S.; Boriano, A.; Bourhaleb, F.; Cirio, R.; Donetti, M.; Fidanzio, A.; Garelli, E.; Giordanengo, S.; Madon, E.; Marchetto, F.; et al. Dosimetric characterization of a large area pixel-segmented ionization chamber. *Med. Phys.* **2004**, *31*, 414–420. [[CrossRef](#)]
4. Létourneau, D.; Gulam, M.; Yan, D.; Oldham, M.; Wong, J.W. Evaluation of a 2D diode array for IMRT quality assurance. *Radiother. Oncol.* **2004**, *70*, 199–206. [[CrossRef](#)] [[PubMed](#)]
5. Létourneau, D.; Publicover, J.; Kozelka, J.; Moseley, D.J.; Jaffray, D.A. Novel dosimetric phantom for quality assurance of volumetric modulated arc therapy. *Med. Phys.* **2009**, *36*, 1813–1821. [[CrossRef](#)]
6. Poppe, B.; Stelljes, T.; Looe, H.; Chofor, N.; Harder, D.; Willborn, K. Performance parameters of a liquid filled ionization chamber array. *Med. Phys.* **2013**, *40*, 082106. [[CrossRef](#)]
7. Markovic, M.; Stathakis, S.; Mavroidis, P.; Jurkovic, I.A.; Papanikolaou, N. Characterization of a two-dimensional liquid-filled ion chamber detector array used for verification of the treatments in radiotherapy. *Med. Phys.* **2014**, *41*, 051704. [[CrossRef](#)] [[PubMed](#)]
8. Van Esch, A.; Basta, K.; Evrard, M.; Ghislain, M.; Sergent, F.; Huyskens, D.P. The Octavius1500 2D ion chamber array and its associated phantoms: Dosimetric characterization of a new prototype. *Med. Phys.* **2014**, *41*, 091708. [[CrossRef](#)]
9. Stelljes, T.; Harmeyer, A.; Reuter, J.; Looe, H.; Chofor, N.; Harder, D.; Poppe, B. Dosimetric characteristics of the novel 2D ionization chamber array OCTAVIUS Detector 1500. *Med. Phys.* **2015**, *42*, 1528–1537. [[CrossRef](#)] [[PubMed](#)]
10. Houweling, A.; De Vries, J.; Wolthaus, J.; Woodings, S.; Kok, J.; Van Asselen, B.; Smit, K.; Bel, A.; Lagendijk, J.; Raaymakers, B. Performance of a cylindrical diode array for use in a 1.5 T MR-linac. *Phys. Med. Biol.* **2016**, *61*, N80. [[CrossRef](#)]
11. King, R.; Agnew, C.; O'Connell, B.; Prise, K.; Hounsell, A.; McGarry, C. Time-resolved dosimetric verification of respiratory-gated radiotherapy exposures using a high-resolution 2D ionisation chamber array. *Phys. Med. Biol.* **2016**, *61*, 5529. [[CrossRef](#)] [[PubMed](#)]

12. Togno, M.; Wilkens, J.; Menichelli, D.; Oechsner, M.; Perez-Andujar, A.; Morin, O. Development and clinical evaluation of an ionization chamber array with 3.5 mm pixel pitch for quality assurance in advanced radiotherapy techniques. *Med. Phys.* **2016**, *43*, 2283–2294. [[CrossRef](#)]
13. Brualla-González, L.; Vázquez-Luque, A.; Zapata, M.; González-Castaño, D.M.; Luna-Vega, V.; Guiu-Souto, J.; Prieto-Pena, J.; García, T.; Granero, D.; Vicedo, A.; et al. Development and clinical characterization of a novel 2041 liquid-filled ionization chambers array for high-resolution verification of radiotherapy treatments. *Med. Phys.* **2018**, *45*, 1771–1781. [[CrossRef](#)]
14. Tölili, H.; Sjögren, R.; Wendelsten, M. A two-dose-rate method for general recombination correction for liquid ionization chambers in pulsed beams. *Phys. Med. Biol.* **2010**, *55*, 4247. [[CrossRef](#)]
15. Andersson, J.; Kaiser, F.J.; Gómez, F.; Jäkel, O.; Pardo-Montero, J.; Tölili, H. A comparison of different experimental methods for general recombination correction for liquid ionization chambers. *Phys. Med. Biol.* **2012**, *57*, 7161. [[CrossRef](#)] [[PubMed](#)]
16. Kry, S.F.; Popple, R.; Molineu, A.; Followill, D.S. Ion recombination correction factors () for Varian TrueBeam high-dose-rate therapy beams. *J. Appl. Clin. Med. Phys.* **2012**, *13*, 318–325. [[CrossRef](#)]
17. Ashraf, M.; Rahman, M.; Zhang, R.; Williams, B.; Gladstone, D.; Pogue, B.; Bruza, P. Dosimetry for FLASH Radiotherapy: A Review of Tools and the Role of Radioluminescence and Cherenkov Emission. *Front. Phys.* **2020**, *8*, 328. [[CrossRef](#)]
18. Szpala, S.; Huang, V.; Zhao, Y.; Kyle, A.; Minchinton, A.; Karan, T.; Kohli, K. Dosimetry with a clinical linac adapted to FLASH electron beams. *J. Appl. Clin. Med. Phys.* **2021**, *22*, 50–59. [[CrossRef](#)] [[PubMed](#)]
19. Boag, J. The recombination correction for an ionisation chamber exposed to pulsed radiation in a 'swept beam' technique. I. Theory. *Phys. Med. Biol.* **1982**, *27*, 201. [[CrossRef](#)]
20. Palmans, H.; Thomas, R.; Duane, S.; Sterpin, E.; Vynckier, S. Ion recombination for ionization chamber dosimetry in a helical tomotherapy unit. *Med. Phys.* **2010**, *37*, 2876–2889. [[CrossRef](#)]
21. Boag, J. Ionization measurements at very high intensities—Part I. *Br. J. Radiol.* **1950**, *23*, 601–611. [[CrossRef](#)]
22. DeBlois, F.; Zankowski, C.; Podgorsak, E.B. Saturation current and collection efficiency for ionization chambers in pulsed beams. *Med. Phys.* **2000**, *27*, 1146–1155. [[CrossRef](#)] [[PubMed](#)]
23. Pardo-Montero, J.; Gómez, F. Determining charge collection efficiency in parallel-plate liquid ionization chambers. *Phys. Med. Biol.* **2009**, *54*, 3677. [[CrossRef](#)]
24. Boag, J.W.; Hochhäuser, E.; Balk, O.A. The effect of free-electron collection on the recombination correction to ionization measurements of pulsed radiation. *Phys. Med. Biol.* **1996**, *41*, 885–897. [[CrossRef](#)] [[PubMed](#)]
25. Brualla-González, L.; Aguiar, P.; González-Castaño, D.; Gómez, F.; Roselló, J.; Pombar, M.; Pardo-Montero, J. Recombination in liquid-filled ionization chambers beyond the Boag limit. *Med. Phys.* **2016**, *43*, 4142–4149. [[CrossRef](#)]
26. Greening, J. Saturation characteristics of parallel-plate ionization chambers. *Phys. Med. Biol.* **1964**, *9*, 143. [[CrossRef](#)]
27. Katoh, K.; Greening, J. On Greening's treatment of saturation characteristics of parallel-plate ionization chambers. *Phys. Med. Biol.* **1965**, *10*, 565. [[CrossRef](#)]
28. Almond, P.R. Use of a Victoreen 500 electrometer to determine ionization chamber collection efficiencies. *Med. Phys.* **1981**, *8*, 901–904. [[CrossRef](#)]
29. Zankowski, C.; Podgorsak, E.B. Determination of saturation charge and collection efficiency for ionization chambers in continuous beams. *Med. Phys.* **1998**, *25*, 908–915. [[CrossRef](#)]
30. Andersson, J.; Tölili, H. Application of the two-dose-rate method for general recombination correction for liquid ionization chambers in continuous beams. *Phys. Med. Biol.* **2010**, *56*, 299. [[CrossRef](#)]
31. Petersson, K.; Jaccard, M.; Germond, J.F.; Buchillier, T.; Bochud, F.; Bourhis, J.; Vozenin, M.C.; Bailat, C. High dose-per-pulse electron beam dosimetry—A model to correct for the ion recombination in the Advanced Markus ionization chamber. *Med. Phys.* **2017**, *44*, 1157–1167. [[CrossRef](#)] [[PubMed](#)]